UNIVERSITY OF CALIFORNIA, BERKELEY
Department of Materials Science and Mineral Engineering

Final Technical Report
to
U.S. Air Force Office of Scientific Research/NA
on

MICROMECHANISMS OF CRACK GROWTH IN LAMINATED INTERMETALLIC COMPOSITE MICROSTRUCTURES

AASERT Grant No. F49620-93-1-0441
supplement to Grant No. F49620-93-1-0107

for period 1 September 1993 to 30 September 1996

by

D. R. Bloyer, K. T. Venkateswara Rao and R. O. Ritchie

November 1996

Report No. UCB/R/96/A1122

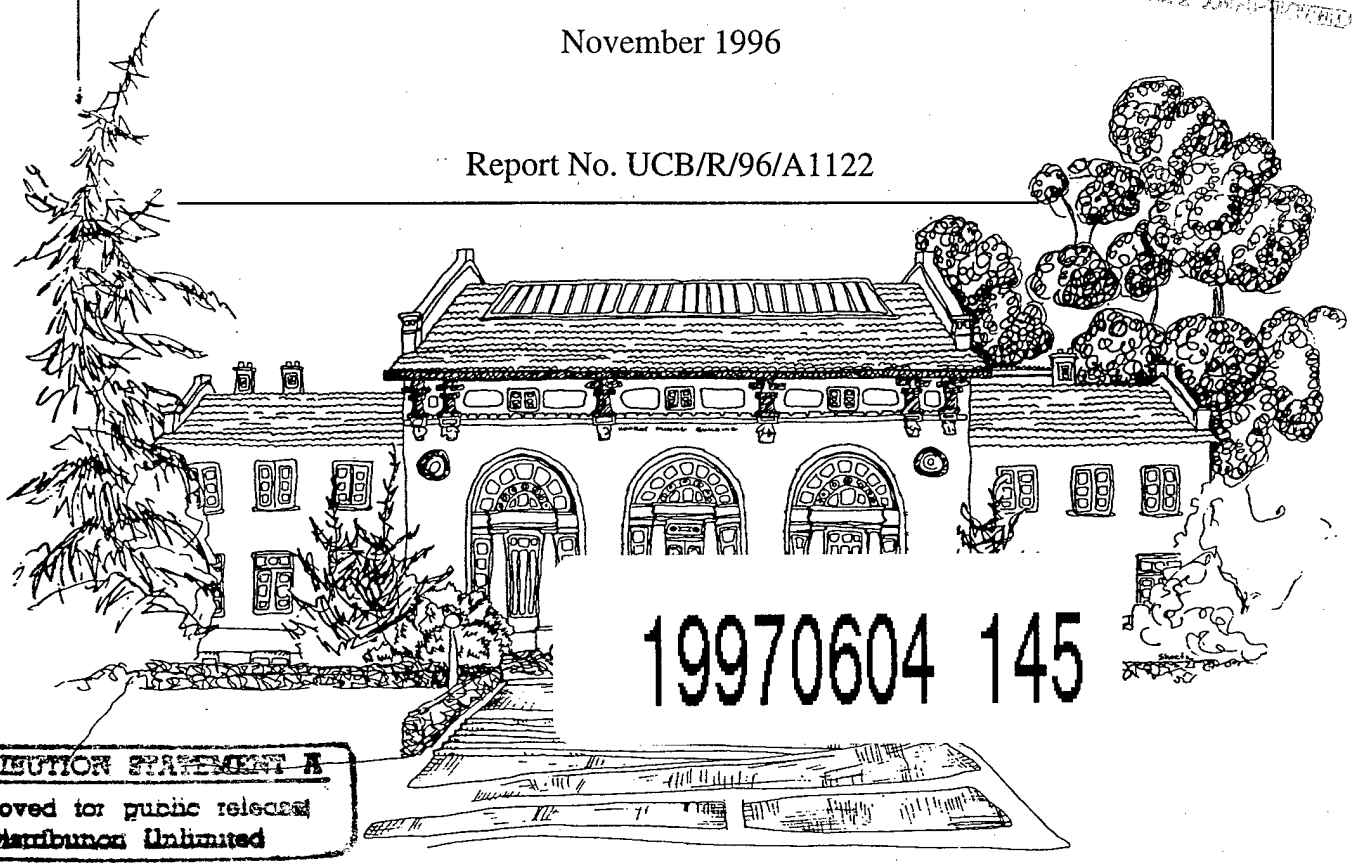

Hearst Mining Building, Berkeley, CA 94720

UNCLASSIFIED
SECURITY CLASSIFICATION OF THIS PAGE

REPORT DOCUMENTATION PAGE

1a. REPORT SECURITY CLASSIFICATION Unclassified	1b. RESTRICTIVE MARKINGS None
2a. SECURITY CLASSIFICATION AUTHORITY Not Applicable	3. DISTRIBUTION/AVAILABILITY OF REPORT ~~Not applicable~~ Unlimited
2b. DECLASSIFICATION/DOWNGRADING SCHEDULE Not applicable	
4. PERFORMING ORGANIZATION REPORT NUMBER(S) UCB/R/96/A1122	5. MONITORING ORGANIZATION REPORT NUMBER(S)
6a. NAME OF PERFORMING ORGANIZATION Robert O. Ritchie, Dept. of Materials Science & Mineral Engineering 6b. OFFICE SYMBOL (If applicable)	7a. NAME OF MONITORING ORGANIZATION Air Force Office of Scientific Research AFOSR/NA
6c. ADDRESS (City, State, and ZIP Code) University of California at Berkeley Evans Hall, MD 1760 Berkeley, California 94720-1760	7b. ADDRESS (City, State, and ZIP Code) 110 Duncan Avenue Room B115 Bolling AFB, DC 20332-8080 ATTN: Dr. C. H. Ward
8a. NAME OF FUNDING/SPONSORING ORGANIZATION AFOSR 8b. OFFICE SYMBOL (If applicable) NA	9. PROCUREMENT INSTRUMENT IDENTIFICATION NUMBER F49620-93-1-0441
8c. ADDRESS (City, State, and ZIP Code) Same as 7a	10. SOURCE OF FUNDING NUMBERS PROGRAM ELEMENT NO. / PROJECT NO. 3484 / TASK NO. XS / WORK UNIT ACCESSION NO.

11. TITLE (Include Security Classification)
MICROMECHANISMS OF CRACK GROWTH IN LAMINATED INTERMETALLIC COMPOSITE MICROSTRUCTURES

12. PERSONAL AUTHOR(S)
BLOYER, D. R., VENKATESWARA RAO, K. T. and RITCHIE, R. O.

13a. TYPE OF REPORT	13b. TIME COVERED	14. DATE OF REPORT (Year, Month, Day)	15. PAGE COUNT
Final	FROM 93/9/1 TO 96/9/31	1996 November 1	25

16. SUPPLEMENTARY NOTATION

17. COSATI CODES			18. SUBJECT TERMS (Continue on reverse if necessary and identify by block number)
FIELD	GROUP	SUB-GROUP	Intermetallic Composites; Fracture Toughness; Fatigue Crack Propagation; Laminates

19. ABSTRACT (Continue on reverse if necessary and identify by block number)

A brittle intermetallic, Nb_3Al, reinforced with a ductile metal, Nb, has been the focus of a study of the resistance curve (R-curve) and cyclic fatigue-crack growth behavior of relatively coarse laminated composites. With the addition of ~50-125 μm thick Nb layers, the toughness of Nb_3Al was increased from ~1 MPa$\sqrt{m}$ to well over 20 MPa$\sqrt{m}$ (after several millimeters of stable crack growth), which was attributed to extensive crack bridging and plastic deformation within unbroken metal phase in the crack wake. The thicker layers provided the best crack-growth resistance although the orientation of these layers, i.e., crack arrester vs. crack divider, did not have a significant effect on toughness properties. Cyclic fatigue-crack growth resistance was also found to be superior in the laminate microstructures compared to monolithic Nb_3Al and Nb-particulate reinforced Nb_3Al composites. Unlike R-curve behavior, however, both layer thickness and orientation significantly affected cyclic crack-growth rates with the crack-arrester orientations displaying the best properties (superior even to monolithic niobium). In general, the optimal combination of fracture toughness and fatigue resistance was seen in the laminates with the thicker Nb layers aligned in the crack arrester orientation.

20. DISTRIBUTION/AVAILABILITY OF ABSTRACT ☒ UNCLASSIFIED/UNLIMITED ☐ SAME AS RPT. ☐ DTIC USERS	21. ABSTRACT SECURITY CLASSIFICATION Unclassified
22a. NAME OF RESPONSIBLE INDIVIDUAL Robert O. Ritchie	22b. TELEPHONE (Include Area Code) (510) 642-0417 22c. OFFICE SYMBOL

DD FORM 1473, 84 MAR 83 APR edition may be used until exhausted. All other editions are obsolete.

SECURITY CLASSIFICATION OF THIS PAGE
Unclassified

Report No. UCB/R/96/A1122

Final Technical Report

to

U.S. Air Force Office of Scientific Research

on

MICROMECHANISMS OF CRACK GROWTH IN LAMINATED INTERMETALLIC COMPOSITE MICROSTRUCTURES

AASERT Grant No. F49620-93-1-0441
supplement to Grant No. F49620-93-1-0107

for period 1 Sept. 1993 to 31 Sept. 1996

submitted to

U.S. Air Force Office of Scientific Research
Directorate of Aerospace and Materials Research
AFOSR/NA
110 Duncan Avenue, Suite B115
Bolling Air Force Base
Washington, D.C. 20322
Attention: Dr. C. H. Ward

submitted by

D. R. Bloyer, K. T. Venkateswara Rao and R. O. Ritchie
Department of Materials Science and Mineral Engineering
University of California, Berkeley, California 94720

November 1996

TABLE OF CONTENTS

MICROMECHANISMS OF CRACK GROWTH IN LAMINATED INTERMETALLIC COMPOSITE MICROSTRUCTURES

D. R. Bloyer, K. T. Venkateswara Rao and R. O. Ritchie

(AASERT Grant No. F49620-93-1-0441)

FOREWORD

This manuscript constitutes the Final Technical Report for Grant No. F49620-93-1-0441, as a supplement to Grant No. F49620-93-1-0107, administered by the U.S. Air Force Office of Scientific Research, with Dr. C. H. Ward as program manager. The work, covering the period September 1, 1993 through September 31, 1996, was performed under the direction of Dr. K. T. Venkateswara Rao, Research Engineer, and Dr. R. O. Ritchie, Professor of Materials Science, University of California at Berkeley, with Don R. Bloyer as a doctoral graduate student.

ABSTRACT

A brittle intermetallic, Nb_3Al, reinforced with a ductile metal, Nb, has been the focus of a study of the resistance curve (R-curve) and cyclic fatigue-crack growth behavior of relatively coarse laminated composites. With the addition of ~50-125 μm thick Nb layers, the toughness of Nb_3Al was increased from ~1 MPa$\sqrt{m}$ to well over 20 MPa$\sqrt{m}$ (after several millimeters of stable crack growth), which was attributed to extensive crack bridging and plastic deformation within unbroken metal phase in the crack wake. The thicker layers provided the best crack-growth resistance although the orientation of these layers, i.e., crack arrester vs. crack divider, did not have a significant effect on toughness properties. Cyclic fatigue-crack growth resistance was also found to be superior in the laminate microstructures compared to monolithic Nb_3Al and Nb-particulate reinforced Nb_3Al composites. Unlike R-curve behavior, however, both layer thickness and orientation significantly affected cyclic crack-growth rates with the crack-arrester orientations displaying the best properties (superior even to monolithic niobium). In general, the optimal combination of fracture toughness and fatigue resistance was seen in the laminates with the thicker Nb layers aligned in the crack arrester orientation.

MICROMECHANISMS OF CRACK GROWTH IN LAMINATED INTERMETALLIC COMPOSITE MICROSTRUCTURES

1. INTRODUCTION

Intermetallic alloys have generated increasing interest over the past decade as possible replacements for the titanium and nickel-base superalloys currently used in aerospace applications. Their attractive properties include higher melting temperatures and lower densities, which for example provide improved specific creep strength for elevated temperature components in high performance engines [1-4]. Due to their ordered crystal structure, however, most intermetallic compounds are extremely brittle at ambient temperatures, severely limiting their use. To improve their low intrinsic toughness, alloy design and microstructural developments have generally been directed toward promoting extrinsic toughening via crack-tip shielding. Shielding mechanisms primarily act behind the crack tip and locally screen the crack from the applied (far-field) driving force [5,6]; specifically, salient mechanisms for toughening intermetallics include crack deflection and crack bridging from unbroken ductile or brittle reinforcements spanning crack. Several intermetallic- and ceramic-matrix composites have been toughened in this manner, including Co/WC, Al/Al_2O_3, Nb/$MoSi_2$, Al/glass, Mg/glass, Nb/γ-TiAl or TiNb/γ-TiAl, Mo/NiAl, Cr/NiAl, and Nb/Nb_3Al; such composites incorporate reinforcements in the form of particulates [7-12], fibers [13-18], or laminates [19-40].

Laminate reinforcements appear to provide the largest toughness improvements; however, there are still questions regarding the effect of scale of the layered microstructure in these materials. Finer microstructures are typically favored with regard to composite strength as the reinforcement scale limits the physical size of processing defects, whereas coarser microstructures are preferred for fracture resistance as they promote crack path tortuosity which hinders crack growth. Accordingly, it is the intent of the present study to examine the role of shape, size, and orientation of the ductile second phase in a model Nb-reinforced/Nb_3Al laminate under both monotonic and cyclic loading conditions.

2. BACKGROUND

The reinforcement of brittle materials with a ductile phase has been widely used to improve their strength, ductility and damage tolerance. The principle behind such ductile-phase toughening is to promote crack-particle interactions which will generate a zone of bridging ligaments in the crack wake. In addition to the plastic deformation of the ductile phase itself, the ligaments provide closure tractions that restrict crack opening, thereby shielding the crack from the applied (far-field) loads.

For conditions of small-scale bridging where the bridging zone is small relative to crack length and the remaining uncracked ligament, the steady-state toughness, G_{ss}, can be obtained from:

$$G_{ss} = G_o + G_b \tag{1}$$

where the crack-tip shielding is described by G_b, the strain energy release rate induced by the bridging, and G_o is the strain energy release rate for crack initiation in the composite. The latter term is often taken as the matrix toughness, although it can exceed this value when crack trapping by the reinforcement phase requires renucleation of the crack across the phase. G_b can be estimated in terms of the area fraction, f, of reinforcement intercepted by the crack (taken to be equivalent to the volume fraction of second phase), its characteristic cross-sectional size, t, and its the tensile yield strength, σ_o, as [41,42]:

$$G_b = f \cdot t \cdot \sigma_o \cdot \chi \tag{2}$$

where χ is the nondimensional work of rupture, which can be estimated from [13]:

$$\chi = \int_0^{u_c} \frac{\sigma_c(u)\, du}{\sigma_o \cdot t} \tag{3}$$

where $\sigma_c(u)$ is the stress-displacement function for the constrained reinforcement in the matrix and u_c is the critical displacement at the failure of this reinforcement. The effect of these contributions to the shielding term is typically exhibited in the form of resistance curve (R-curve) behavior where the apparent toughness of the material increases with increasing crack length, commensurate with the development of a shielding zone in the crack wake [41,42].

The degree of composite toughening is a marked function of the morphology and properties of the reinforcement and its interface with the matrix (Figs. 1 and 2). For toughening brittle intermetallics and ceramics, higher volume fractions of ductile reinforcement generally result in a larger amount of ductile phase intercepting the crack, thereby, increasing plastic energy dissipated in the crack wake and escalating crack-tip shielding [31,41,42]. High aspect-ratio ductile second phases are generally preferred to particulate (e.g., spherical) reinforcements as they increase the probability of intersection with the crack; provided the reinforcements remain unbroken, this enhances R-curve toughening by creating a larger shielding zone behind the crack tip. The roles of the yield strength and χ are more complex, and in fact, are typically interrelated [13,23]. These parameters are primarily influenced by the constraint in the ductile phase imposed by the surrounding matrix material, and are thus highly dependent on the reinforcement/matrix interfacial properties. Finally, laminate reinforcements offer the additional advantage of an increased initiation toughness as in the arrester orientation, the entire crack front intercepts the reinforcement phase and therefore must renucleate across it. These effects are summarized in Figs. 1 and 2.

Most physical models for crack bridging by ductile reinforcements suggest increased toughening with increased reinforcement thickness [13,23,41,42], but this has yet to be demonstrated experimentally for a laminate with a constant reinforcement volume fraction. Moreover, the majority of the studies to date have focused on the fracture behavior of ductile-layer reinforced composites [19-39]; hardly any attention has been given to their cyclic fatigue properties [28,31,40]. Preliminary studies in γ-TiAl alloys reinforced with β-TiNb [31] indicate that the crack-tip shielding that promotes R-curve toughening under monotonic loading is all but eliminated under cyclic loading conditions; this results from accumulated fatigue damage in the ductile phase leading to premature failure of the bridging ligaments.

Accordingly, in the present study, the fracture and fatigue behavior of a model Nb-reinforced Nb_3Al laminate composite is examined, where toughening is achieved by the addition of ductile Nb layers having layer dimensions in the tens to hundreds of microns. Results are compared with earlier studies on Nb/Nb_3Al composites where the ductile Nb phase was present either as a ~20-μm particulate reinforcement formed *in situ* by powder metallurgy [11,12], or as 2-μm thick (magnetron sputtered) layers in the form of a microlaminate [32,33].

3. EXPERIMENTAL PROCEDURES

The materials studied all consisted of 20 vol.% of Nb layers bonded to Nb_3Al in the form of two laminate orientations and two laminate layers thicknesses. The laminate orientations investigated were:

- a "crack arrester" (0° or C-L) orientation, where the crack grows perpendicular to, yet sequentially through, the layers
- a "crack divider" (C-R) orientation, where the crack plane is normal to the plane of layers, but the crack advances through all the layers simultaneously.

The laminate thicknesses were:

- ~125-μm thick layers of Nb separating 500-μm thick layers of Nb_3Al
- ~50-μm thick layers of Nb separating 200-μm thick layers of Nb_3Al.

These were fabricated by cold compacting Nb_3Al powder between Nb foils and subsequently hot pressing in an argon atmosphere to give dense (>96% of theoretical density) composite cylinders with 20 vol.% Nb. The resultant microstructures consisted of evenly spaced layers of Nb_3Al separated by layers of Nb, as shown in Figure 3.

~125 μm Nb / 500 μm Nb_3Al Laminate: Arrester laminates used in fracture toughness testing were processed at 1680°C for 40 minutes resulting in a reaction zone between the metal- intermetallic layers approximately 20-30 μm in thickness; this equates to an approximate 30-40% reduction in the Nb layer thickness. The arrester fatigue and divider

specimens were processed at 1650°C for 25 minutes reducing the reaction layer to only approximately 20-25% of the Nb layer.

Fatigue pre-cracked single-edged notched bend SEN(B) beams (with span ~35 - 40 mm, thickness B = 3.5 mm, and width W = 12.5 mm) were used to study the resistance curve (R-curve) behavior of the arrester orientation; compact-tension C(T) specimens (with B = 3.5 mm and W = 25.4 mm) were used for the corresponding fatigue testing. Disc-shaped compact-tension DC(T) specimens (with B = 3.2 mm and W = 33 mm) were used for both fracture and fatigue testing in the divider orientation.

~50 μm Nb / 200 μm Nb_3Al Laminate: Corresponding divider specimens were processed at 500°C for 25 minutes resulting in a Nb layer thickness reduction of approximately 20-25%. Both R-curve and fatigue tests were performed using DC(T) specimens (with B = 4.0 mm and W = 33 mm).

4. RESULTS AND DISCUSSION

4.1 Fracture Toughness and R-Curve Behavior

The R-curve results, plotted in Figure 4a for the divider orientation, illustrate that the addition of high aspect-ratio ductile reinforcements leads to significant improvements in the fracture toughness of Nb_3Al. Compared to an intrinsic toughness of only ~1 MPa$\sqrt{m}$ for unreinforced Nb_3Al, the addition of 20 vol.% of ~50-μm thick Nb layers resulted in a crack-initiation toughness of ~6 MPa$\sqrt{m}$ and a crack-growth toughness exceeding 10 MPa$\sqrt{m}$; the ~125-μm layers of Nb yielded even better properties with an initiation toughness of 7-9 MPa$\sqrt{m}$ and a growth toughness of over 20 MPa$\sqrt{m}$.

It should be noted that the present laminates contain only 20 vol% Nb, yet they exhibit markedly higher toughness than Nb particulate toughened Nb_3Al which contains twice as much Nb [12] (Fig. 4b). Moreover, they display superior toughness properties to a microlaminate consisting of ~2-μm thick Nb layers in Nb_3Al; this material contained ~50 vol.% Nb, but displayed initiation and growth toughnesses of only ~6 and 10 MPa$\sqrt{m}$, respectively [32,33]. For the latter material, quasi-static crack extension occurred only over the first 200 μm of growth; by contrast, the present laminates with ~50 μm and 125-μm thick Nb layers, exhibited stable cracking over crack extensions of 2-3 mm.

It is clear that the laminates with coarser Nb layers require far less reinforcement to achieve significantly improved fracture toughness properties; indeed, compared with particulate or microlaminate reinforcement, the crack-initiation toughness, the maximum crack-growth toughness and the extent of subcritical cracking prior to instability are all enhanced.

The highest toughness properties in the present coarser-scale laminates were seen in the arrester orientation (Fig. 5). With ~125-μm thick Nb layers in this orientation, an initiation toughness of ~9 MPa$\sqrt{m}$ was seen; furthermore, in certain samples, crack-growth toughnesses as high as ~70 MPa$\sqrt{m}$ were observed. Although the arrester orientations were clearly tougher than corresponding divider orientations, the effect of laminate orientation on R-curve properties was not large; indeed, there was significant overlap of the data between the two orientations.

Mechanistically the elevation in crack-initiation toughness in the coarse-scale laminates can be related to crack renucleation across the Nb layer (in the arrester orientation); thereafter, crack-growth toughness on the R-curve is associated with crack bridging and plastic deformation in the Nb ligaments. The rapid increase in toughness at larger crack extensions, e.g., at stress intensities above ~30 MPa$\sqrt{m}$, is caused by large-scale bridging, where the size of the crack-wake shielding zone becomes comparable to the crack size and specimen dimensions. In this regime, the toughness becomes geometry sensitive.

4.2 Crack/Layer Interactions

Arrester Laminates: Extensive metallography showed that the development of the R-curve is associated with significant crack-reinforcement interactions, involving crack arrest at the Nb layer and crack renucleation ahead of the layer [38-40]. Typically the crack impinges on a reinforcing layer, blunts, and renucleates across the layer with increasing applied stress intensity. This process recurs as the crack advances across several Nb layers leaving them intact; this in turn leads to the formation of large (~3-6 mm) bridging zones in the crack wake. Crack branching on one or both sides of the Nb layer commonly occurs in the matrix near the Nb/Nb_3Al interface, but not necessarily at the interface. The branches then link up to form a single dominant crack as the crack progressed across the specimen. Such near interfacial cracking resulted in effective debonding at the Nb/Nb_3Al interface, thus relieving constraint and promoting ductile failure in the Nb layer [13,23]. Consequently, when near interfacial cracking occurred and constraint was relieved, the Nb layer failed by microvoid coalescence; conversely, when near interfacial cracking was not observed, the constraint imposed on the layer promoted cleavage fracture of the Nb.

Divider Laminates: Crack/layer interactions in divider samples were analogous to those observed in arrester samples, except for the fact that in the latter orientation, crack arrest occurred at the Nb layer. Specifically, near interfacial cracking was more frequent in the divider laminates than was typically seen in the arrester material. During R-curve measurement, it was observed that a single crack grew stably over a few millimeters and appeared to arrest; however, upon further loading an extensive microcrack zone developed ahead of the crack tip. At this point, R-curve measurements were halted.

4.3 Models for Toughening

Most models for ductile-phase toughening pertain to small-scale bridging (SSB) conditions, where the bridging zone is small relative to the crack length and remaining uncracked ligament in the sample. However, because large-scale bridging conditions prevailed in the present series of experiments, both small-scale and large-scale bridging models are used below to evaluate the role of layered Nb reinforcements on the fracture toughness of Nb/Nb_3Al laminates.

Bridging models typically require two experimental parameters to estimate the nondimensional work of rupture, χ, namely the stress-displacement function, $\sigma_c(u)$, for the constrained reinforcement in the matrix, and the critical displacement, u_c, at the failure of this reinforcement. Using the approach described in Eq. 1-3, the extent of toughening can be expressed in terms of stress intensities, as [41,42]:

$$K_{ss} = \sqrt{K_o^2 + E' f \sigma_o t \chi} \tag{4}$$

where K_o and K_{ss} are respectively the crack initiation and crack growth (or steady-state) toughnesses.

To evaluate Eqs. 1-4, we note that values of χ between 1.3-2.5 [21] have been reported for Nb/TiAl and $Nb/MoSi_2$ laminates of similar microstructural scale; as these values were influenced by small amounts of debonding, a conservative value of $\chi \sim 1.3$ is assumed here. For the arrester laminate where $K_o \sim 9$ MPa$\sqrt{m}$ (Fig. 5), $f \sim 0.2$, plane strain composite modulus, $E' = 142$ GPa (assuming $E_{composite} = 129$ GPa and $\nu \sim 0.3$), the flow stress of Nb, $\sigma_o \sim 245$ MPa [43], and the half thickness of the ~125-μm thick Nb layer, $t \sim 62.5$ μm, Eq. 4 predicts a steady-state toughness of ~25 MPa$\sqrt{m}$ for the laminate with ~125-μm thick Nb layers, in reasonable agreement with the measured plateau toughness (Fig. 4a). If allowance is made for the reduction in t and f due to the presence of the reaction layer, the predicted toughness is somewhat lower (~18 MPa$\sqrt{m}$); for comparison, a similar analysis of the divider laminate with ~50-μm thick Nb layers gave a corrected value of ~13 MPa$\sqrt{m}$.

An alternative approach uses the stress-intensity solution for a point load behind the crack tip in an edge crack specimen and assumes a traction function to describe the bridging zone [15]. This function is then integrated with the appropriate weighting function to determine the shielding contribution of the bridges. The far-field stress intensity at steady state, K_{ss}, can be computed by superposition of the crack-tip stress intensity, K_o, and the shielding stress intensity imparted by the tractions, K_b, given as:

$$K_b = \frac{2}{\sqrt{\pi a}} \int_0^L \sigma(x) F\left(\frac{x}{a}, \frac{a}{W}\right) dx \tag{5}$$

where a is the crack length, x is the distance behind the crack tip, W is the specimen width, L is the bridging zone length, $\sigma(x)$ is a stress function describing the tractions in the wake, and the geometric weight function F is given in refs. [15,39,44].

For large-scale bridging (LSB) conditions, Eq. 5 can be used directly, although predictions are complicated by the fact that the R-curve is also dependent on specimen geometry. A rigorous modeling approach requires the use of the exact stress-displacement function ($\sigma_c(u)$) and crack-opening profile ($u(x)$) for the specific geometry [25]. However, assuming uniform tractions ($\sigma(x) = f\sigma_o$) and weight function, F, developed for single-edge notched samples [15,44], a simple estimate for the R-curve under large-scale bridging conditions can be obtained by integrating Eq. 5 at various crack-growth increments and superimposing the toughening increment, K_b, onto the intrinsic crack-tip stress intensity K_o. The prediction for the arrester laminate with 125-μm thick Nb layers is shown in Figure 5 for crack extension of up to a final bridging zone length of 5 mm. Although the simple model underpredicts the toughness, the calculations are consistent with the observed trend for crack-growth toughness (increasing slope and positive curvature) under large-scale bridging conditions.

In the limit of L/a and $L/(W-a)$ approaching zero, the weight function reduces to $(a/2x)^{1/2}$, in agreement with previous analyses using rigid-plastic spring models [41,42]; as before, a small-scale bridging limit can be extracted applying the same simplifying assumptions to the traction function. For the arrester laminate with 125-μm thick Nb layers, the predicted SSB limit was ~12 MPa$\sqrt{m}$, which is considerably lower than the toughness observed from the R-curve.

Neither of these models provide close estimates of the R-curve behavior of these laminates, presumably because of the simplifying assumptions concerning the traction function, $\sigma(x)$. More accurate estimations of this function, or preferably actual measurements, are necessary for the contribution of bridging to the development of the R-curve to be modeled precisely.

4.4 Fatigue-Crack Propagation Behavior

Fatigue-crack propagation rates for both the divider and arrester laminates with 125-μm thick Nb layers are compared to corresponding behavior in the Nb particulate reinforced Nb_3Al [11] in Figure 6. The cyclic crack-growth properties of Nb_3Al are clearly improved by ductile reinforcement. Compared to an increase in the ΔK_{TH} fatigue threshold from ~1 to ~2 MPa$\sqrt{m}$ through the incorporation of particulate reinforcements, thresholds above 4 MPa$\sqrt{m}$ are seen in the divider laminates and approach 6 MPa$\sqrt{m}$ in the arrester laminates.

As the crack is continuously exposed to the intermetallic phase in the particulate reinforced and the divider laminate, their crack-growth curves might be expected to lie between those of the unreinforced matrix and pure Nb. However, from Figure 6 it is

apparent that the high aspect ratio of the laminate reinforcement results in a significantly higher threshold.

Mechanistically, the fatigue-crack growth properties of the laminates are markedly affected by the fact that crack bridging from the Nb layers, which is primarily responsible for the R-curve toughening under monotonic loads, is reduced under cyclic loading due to premature fatigue failure of the metallic bridging ligaments. This is illustrated in Figure 7 where the failure of the reinforcing layers under fatigue loading occurs with little gross plastic deformation compared to corresponding behavior under monotonic loading conditions [11,31]. This phenomenon is quite common in ductile-particle reinforced intermetallic composites, where the principal effect of the fatigue loading is to degrade the toughening mechanisms [11,18,24,31].

Figure 6 also demonstrates the effect of layer orientation on the fatigue properties of the laminate. The arrester orientation, where the crack tip resides entirely in either the matrix or the reinforcement during crack extension, shows the best fatigue resistance compared to the particulate and divider laminate composites (which have a continuous matrix). At lower ΔK values, growth rates are comparable to rates in monolithic Nb since the maximum stress intensity, K_{max}, is not large enough to reinitiate the crack across the reinforcing layer. The crack thus remains trapped in the layer where it can induce fatigue damage and reinforcement failure before appreciable crack bridging can develop (Figure 8a). However, at higher applied ΔK values where K_{max} approaches K_o, the crack-initiation toughness of the composite, the crack is now able to reinitiate across the layer (Figure 8b); this allows the formation of an intact bridge which contributes to crack-tip shielding which in turn results in growth rates that are significantly slower than in either the Nb or Nb_3Al constituents. Thus, it appears that the fatigue-induced degradation of ductile-phase bridging is less pronounced in the arrester laminates; this results in a fatigue-crack propagation resistance superior to any Nb/Nb_3Al composites examined to date, and in fact superior to metallic niobium.

Figure 9 shows the effect of Nb layer thickness on fatigue-crack growth behavior in the divider laminates at $R = 0.1$ and 0.5. It is apparent that at both load ratios, the laminate with the larger metallic layer thickness displays the best fatigue-crack growth rates; specifically, the ΔK_{TH} threshold at $R = 0.1$ is raised from under 4 to ~5 MPa$\sqrt{m}$ by increasing the Nb layer thickness from 50 to 125 μm. Unlike behavior in metals and ceramics [45], the growth rates in the laminates are not normalized by plotting in terms of ΔK or K_{max}; such behavior is typical of intermetallic alloys and reflects the fact that fatigue-crack growth in these materials is essentially equally affected by *intrinsic* damage mechanisms *ahead* of the crack tip and *extrinsic* shielding mechanisms *behind* the tip. In terms of a modified Paris power-law relationship expressed in terms of ΔK and K_{max}, viz: [46]

$$da / dN \propto \Delta K^n K_{max}^p \qquad (6)$$

the ΔK and K_{max} dependencies are $n = 3$ and $p = 7$ for the 50-μm thick Nb laminate and $n = 3$ and $p = 8$ for the 125-μm thick material. This is in contrast to metallic alloys where invariably $n \gg p$ and in non-transforming ceramics where conversely $n \ll p$.

Although there were no obvious mechanistic differences in the cracking behavior in the two layer thickness, some indirect observations indicate the origin of the differences in growth rates. Compliance-based estimates of the crack length in both divider laminate thicknesses tended to underestimate the crack length, as measured by *in situ* optical observation, particularly at the higher applied stress-intensity ranges. This generally is evidence of the existence of a small bridging zone behind the crack tip. Measurements indicated that the effect was more pronounced in the 125-μm thick Nb laminate, suggesting that the bridging zones were more significant with the thicker Nb layers. This implies that the effect of layer thickness on fatigue-crack growth rates is associated with the bridging zone that develops as the crack tunnels ahead in the intermetallic layers, leaving small ligaments of intact Nb metal in the crack wake.

5. CONCLUSIONS

Based on a study of the fracture toughness/resistance-curve and fatigue-crack propagation behavior of ductile Nb-reinforced Nb_3Al intermetallic-matrix (coarse-scale) laminates, the following conclusions can be made:

- The incorporation of high aspect ratio, coarse-scale, metallic reinforcements in the form of laminate structures provides for significant toughening in Nb_3Al; optimal toughness was achieved with the thicker (~125 μm) Nb layers. Compared to an intrinsic toughness of ~1 MPa$\sqrt{m}$ for monolithic Nb_3Al, crack-initiation toughnesses of K_o ~ 7-8 MPa$\sqrt{m}$ and growth toughnesses of K_{ss} ~12 MPa$\sqrt{m}$ were measured for the 50-μm Nb/200-μm Nb_3Al divider laminates and values of K_o ~ 9 MPa$\sqrt{m}$ and K_{ss} ~ 20 MPa$\sqrt{m}$ for the 125-μm Nb/500-μm Nb_3Al material. Such toughening was found to be associated with the development of significant crack bridging by intact Nb layers in the crack wake which act to shield the crack tip. Although the effect of layer orientation, i.e., arrester vs. divider, was not large, the arrester orientation did display higher crack-growth toughnesses.

- Under cyclic fatigue loading, resistance to fatigue-crack growth was markedly superior in the laminates compared to monolithic Nb_3Al and particulate reinforced Nb_3Al; indeed growth-rate properties in the arrester laminates were comparable, and at higher growth rates even better than in monolithic Nb. Despite the improved fatigue properties, mechanistically a degradation in toughening was observed under cyclic loading, resulting from the premature fatigue failure of the Nb phase; however, the effect was dependent upon the laminate orientation. Reinforcement layer thickness had an equally pronounced effect under cyclic loading with thicker layers providing improved fatigue resistance. The slower growth rates in the thicker laminates was

attributed to the existence of small bridging zones which were retained under cyclic loads.

6. ACKNOWLEDGMENTS

This work was funded by the Air Force Office of Scientific Research under the AASERT Program (Grant # F49620-93-1-0441) as a supplement to Grant # F49620-93-1-0107. The authors wish to thank Dr. C. H. Ward for his support and Drs. B. J. Dalgleish and L. C. DeJonghe for help with the processing.

7. REFERENCES

1. R.T. Fleischer, "Mechanical Properties of Diverse High-Temperature Compounds-Thermal Variation of Microhardness and Crack Formation," in *High Temperature Ordered Intermetallic Alloys III*, C.T. Liu, *et al.*, eds., Materials Research Society. Pittsburgh, PA, 1989, pp. 305-310.

2. D.L. Anton and D.M. Shah, "Mechanical Properties of Diverse High-Temperature Compounds--Thermal Variation of Microhardness and Crack Formation," in *High Temperature Ordered Intermetallic Alloys III*," C.T. Liu, *et al.*, eds., Materials Research Society. Pittsburgh, PA, 1989, pp. 361-371.

3. D.L. Anton and D.M. Shah, "Ductile Phase Toughening of Brittle Intermetallics," in *Intermetallic Matrix Composites*, D.L. Anton, *et al.*, eds., Materials Research Society. Pittsburgh, PA, 1990, pp. 45-52.

4. D.M. Shah, D.L. Anton, and C.W. Musson, "Feasibility Study of Intermetallic Composites," in *Intermetallic Matrix Composites*, D.L. Anton, *et al.*, eds., Materials Research Society. Pittsburgh, PA, 1990, pp. 333-340.

5. A.G. Evans, "Perspective on the Development of High-Toughness Ceramics," *J. Am. Ceram. Soc.* **72** (2), 187-206 (1990).

6. R.O. Ritchie, "Mechanisms of Fatigue Crack Propagation in Metals, Ceramics and Composites: Role of Crack Tip Shielding," *Mater. Sci. Eng. A* **A103**, 15-28 (1988).

7. V.V. Krstic, P.S. Nicholson, and R.G. Hoagland, "Toughening of Glasses by Metallic Particles," *J. Am. Ceram. Soc.* **64** (9), 499-504 (1981).

8. L.S. Sigl, P.A. Mataga, B.J. Dalgleish, R.M. McMeeking, and A.G. Evans, "On the Toughness of Brittle Materials Reinforced with a Ductile Phase," *Acta metall.* **36** (4), 945-953 (1988).

9. P.A. Mataga, "Deformation of Crack-Bridging Ductile Reinforcements in Toughened Brittle Materials," *Acta metall.* **37** (12), 3349-3359 (1989).

10. K.T. Venkateswara Rao, W.O. Soboyejo, and R.O. Ritchie, "Ductile-Phase Toughening and Fatigue-Crack Growth in Nb-Reinforced Molybdenum Disilicide Intermetallic Composites," *Metall. Trans. A* **23A**, 2249-2257 (1992).

11. L. Murugesh, K.T. Venkateswara Rao, and R.O. Ritchie, "Crack Growth in a Ductile-Phase-Toughened Nb/Nb_3Al In Situ Intermetallic Composite Under Monotonic and Cyclic Loading," *Scripta Metall. Mater.* **29**, 1107-1112 (1993).

12. C.D. Bencher, A. Sakaida, K.T. Venkateswara Rao, and R.O. Ritchie, "Toughening Mechanisms in Ductile Niobium Reinforced Niobium Aluminide (Nb/Nb_3Al) *In Situ* Composites," *Metall. Mater. Trans. A* **26A**, 2027-2033 (1995).

13. M.F. Ashby, F.J. Blunt, and M. Bannister, "Flow Characteristics of Highly Constrained Metal Wires," *Acta metall.* **37** (7), 1847-1857 (1989).

14. H.C. Cao, B.J. Calgleish, H.E. Dève, E. Elliot, A.G. Evans, R. Mehrabian, and G. R. Odette., "A Test Procedure for Characterizing the Toughening of Brittle Intermetallics by Ductile Reinforcements," *Acta metall.* **37** (11), 2969-2977 (1989).

15. F. Zok and C.L. Hom, "Large Scale Bridging in Brittle Matrix Composites," *Acta metall. mater.* **38** (10), 1895-1904 (1990).

16. B.D. Flinn, C.S. Lo, F.W. Zok, and A.G. Evans, "Fracture Resistance Characteristics of a Metal-Toughened Ceramic," *J. Am. Ceram. Soc.* **76** (2), 369-75 (1993).

17. D.E. Alman and N.S. Stoloff, "The Effect of Niobium Morphology on the Fracture Behavior of $MoSi_2/Nb$ Composites," *Metall. Mater. Trans. A* **26A**, 289-303 (1995).

18. K. Badrinarayanan, A.L. McKelvey, K.T. Venkateswara Rao, and R.O. Ritchie, "Fracture and Fatigue-Crack Growth Behavior in Ductile-Phase Toughened Molybdenum Disilicide: Effects of Niobium Wire vs. Paritculate Reinforcements," *Metall. Mater. Trans. A* **28A**, in press (1996).

19. C.K. Elliott, G.R. Odette, G.E. Lucas, and J.W. Sheckhard. "Toughening Mechanisms in Intermetallic γ-TiAl Alloys Containing Ductile Phases," in *High-Temperature/High-Performance Composites*, F.D. Lemkey, *et al.*, eds., Materials Research Society. Pittsburgh, PA, 1988, pp. 95-101.

20. B.J. Dalgleish, K.P. Trumble, and A.G. Evans, "The Strength and Fracture of Alumina Bonded Aluminum Alloys," *Acta metall.* **37** (7), 1923-1931 (1989).

21. H.E. Dève, A.G. Evans, G.R. Odette, R. Mehrabian, M.L. Emiliani, and R.J. Hecht, "Ductile Reinforcement Toughening of γ-TiAl: Effects of Debonding and Ductility," *Acta metall. mater.* **38** (8), 1491-1502 (1990).

22. T.C. Lu, A.G. Evans, R.J. Hecht, and R. Mehrabian, "Toughening of $MoSi_2$ with a Ductile (Niobium) Reinforcement," *Acta metall. mater.* **38** (8), 1853-1862 (1991).

23. M. Bannister and M.F. Ashby, "The Deformation and Fracture of Constrained Metal Sheets," *Acta metall. mater.* **39** (11), 2575-2582 (1991).

24. K.T. Venkateswara Rao, G.R. Odetted, and R.O. Ritchie, "On the Contrasting Role of Ductile-Phase Reinforcements in the Fracture Toughness and Fatigue-Crack Propagation Behavior of TiNb/γ-TiAl Intermetallic Matrix Composites," *Acta metall. mater.* **40** (2), 353-361 (1992).

25. G.R. Odette, B.L. Chao, J.W. Sheckhard, and G.E. Lucas, "Ductile Phase Toughening Mechanism in a TiAl-TiNb Laminate Composite," *Acta metall. mater.* **40** (9), 2381-2389 (1992).

26. F.E. Heredia, M.Y. He, G.E. Lucas, A.G. Evans, H.E. Dève, and D. Kenitzer, "The Fracture Resistance of Directionally Solidified Dual-Phase NiAl Reinforced with Refractory Metals," *Acta metall. mater.* **41** (2), 505-511 (1993).

27. M.Y. He, F.E. Heredia, D.J. Wissuchek, M.C. Shaw, and A.G. Evans, "The Mechanics of Crack Growth in Layered Materials," *Acta metall. mater.* **41** (4), 1223-1228 (1993).

28. W.O. Soboyejo, K.T. Venkateswara Rao, S.M.L. Sastry, and R.O. Ritchie, "Strength, Fracture, and Fatigue Behavior of Advanced High-Temperature Intermetallics Reinforced with Ductile Phases," *Metall. Trans. A* **24A**, 585-599 (1993).

29. W.O. Soboyejo and S.M.L. Sastry, "An Investigation of the Effects of Ductile Phase Reinforcement on the Mechanical Behavior of Advanced High Temperature Intermetallics," *Mater. Sci. Eng.* **A171**, p. 95-104 (1993).

30. M.C. Shaw, D.B. Marshall, M.S. Dadkhah, and A.G. Evans, "Cracking and Damage Mechanisms in Ceramic/Metal Multilayers," *Acta metall. mater.* **41** (11), 3311-3322 (1993).

31. K.T. Venkateswara Rao, G.R. Odette, and R.O. Ritchie, "Ductile-Reinforcement Toughening in γ-TiAl Intermetallic-Matrix Composites: Effects on Fracture Toughness and Fatigue-Crack Propagation Resistance," *Acta metall. mater.* **42** (3), 893-911 (1994).

32. H.C. Cao, J.P. Lofvander, A.G. Evans, R. R.G., and D.W. Skelly, "Mechanical Properties of an *In Situ* Synthesized Nb/Nb_3Al Layered Composite," *Mater. Sci. Eng.* **A185**, 87-95 (1994).

33. R.G. Rowe, D.W.S. Kelly, M. Larsen, J. Heathcote, G. Lucas, and G.R. Odette, "Properties of Microlaminated Intermetallic-Refractory Metal Composites," in *High Temperature Silicides and Refractory Alloys*, C.L. Bryant *et al.*, eds., Materials Research Society, 1993, p. 461.

34. Q. Ma, M.C. Shaw, M.Y. He, D.J. Dalgleish, D.R. Clarke, and A.G. Evans, "Stress Redistribution in Ceramic/Metal Multilayers Containing Cracks," *Acta metall. mater.* **43** (6), 2137-2142 (1995).

35. J. Kajuch, J. Short, and J.J. Lewandowski, "Deformation and Fracture Behavior of Nb in Nb_5Si_3/Nb Laminates and its Effect on Laminate Toughness," *Acta metall. mater.* **43** (5), 1955-1967 (1995).

36. J. Heathcote, G.R. Odette, and G.E. Lucas, "Constrained Metal Deformation in an Intermetallic/Metallic Microlaminate Composite," in *Layered Materials for Structural Applications*, Vol. 434, J.J. Lewandowski *et al.*, eds., Materials Research Society, 1996, in press.

37. J. Heathcote, G.R. Odette, and G.E. Lucas, "On the Micromechanics of Low Temperature Strength and Toughness of Intermetallic/Metallic Microlaminate Composites," *Acta mater.* **44** (11), 4289-4299 (1996).

38. D.R. Bloyer, K.T. Venkateswara Rao and R.O. Ritchie, "Resistance-Curve Toughening in Ductile/Brittle Layered Structures: Behavior in Nb/Nb_3Al Laminates," *Mater. Sci. Eng.* **A216** (1-2), 80-90 (1996).

39. D.R. Bloyer, K.T. Venkateswara Rao and R.O. Ritchie, "Resistance-Curve Toughening in Ductile-Phase Intermetallic Laminates," *in Proc. Johannes Weertman Symposium*, R. J. Arsenault *et al.*, eds., The Minerals, Metals & Materials Society, Warrendale, PA, 1996, in press.

40. D.R. Bloyer, K.T. Venkateswara Rao and R.O. Ritchie, "Toughness and Subcritical Crack Growth in Nb/Nb_3Al Layered Materials," in *Layered Materials for Structural Applications*, Vol. 434, J.J. Lewandowski *et al.*, eds., Materials Research Society Proc., 1996, in press.

41. A.G. Evans and R.M. McMeeking, "On the Toughening of Ceramics by Strong Reinforcements," *Acta metall.* **34** (12), 2435-2441 (1986).

42. B. Budiansky, J.C. Amazigo, and A.G. Evans, "Small-Scale Crack Bridging and the Fracture Toughness of Particulate-Reinforced Ceramics," *J. Mech. Phys. Solids* **36** (2), 167-87 (1988).

43. *ASM Metals Handbook*, Desk Edition., ASM Intl., Materials Park, OH, 1985, p. 14.9.

44. H. Tada, P.C. Paris and G.R. Irwin, in *Stress Analysis of Cracks Handbook*, Del Research Corp./Paris Publ., St. Louis, MO, 1985.

45. R.O. Ritchie and K.T. Venkateswara Rao, "Cyclic Fatigue-Crack Growth in Toughened Ceramics and Intermetallics at Ambient to Elevated Temperatures," in *Mechanisms and Mechanics of Damage and Failure*, Proceedings of the Eleventh European Conference on Fracture, Vol. I, J. Petit, ed., EMAS Ltd., Warley, U.K., 1996, pp. 53-69.

46. R.H. Dauskardt, M.R. James, J.R. Porter, and R.O. Ritchie, "Cyclic Fatigue-Crack Growth in SiC-Whisker-Reinforced Alumina Ceramic Composite: Long and Small-Crack Behavior," *J. Am. Ceram. Soc.* **75** (4), 759-771 (1992).

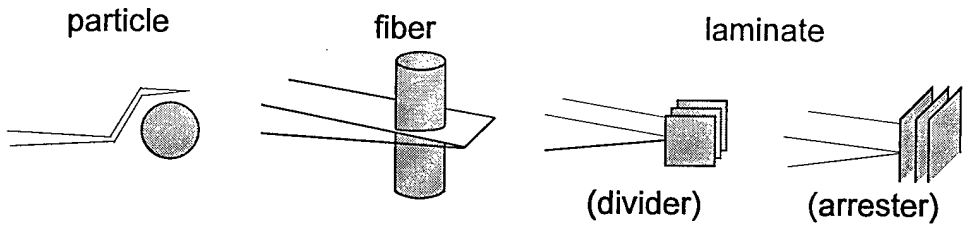

Fig. 1. Various reinforcing morphologies used in composite toughening.

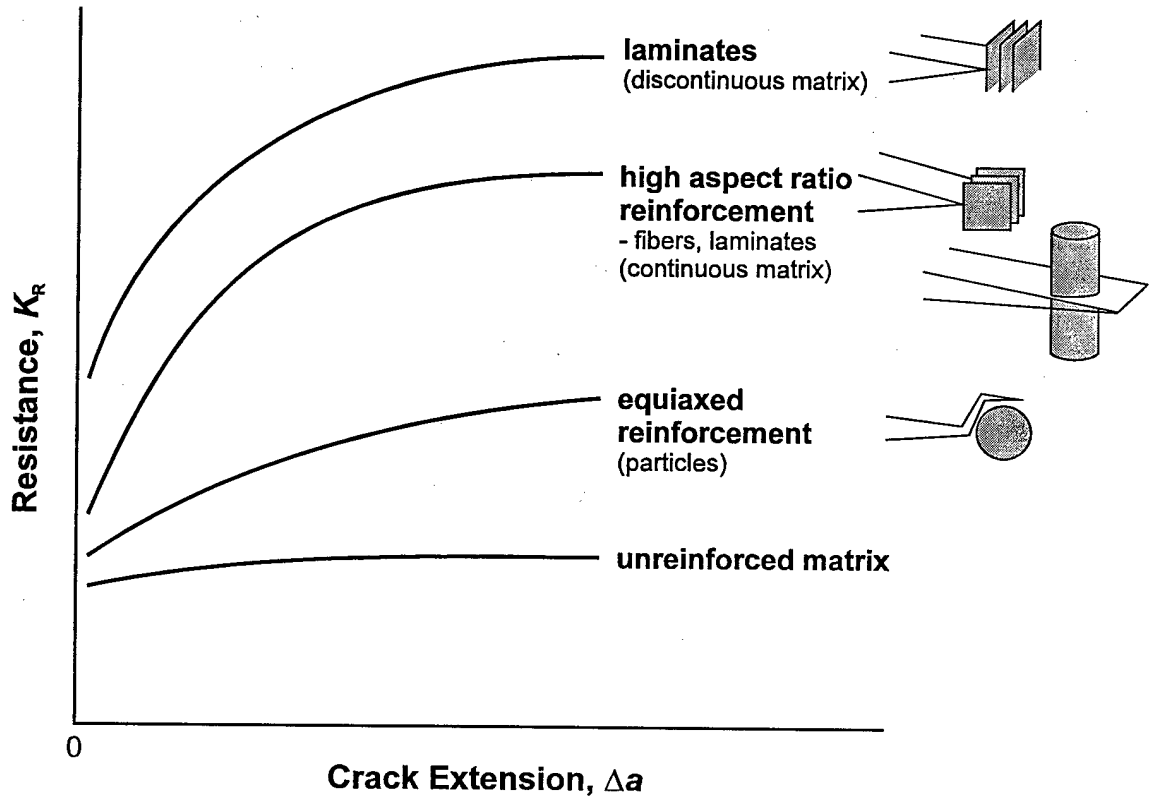

Fig. 2. Trends in achievable toughness for various composite reinforcements.

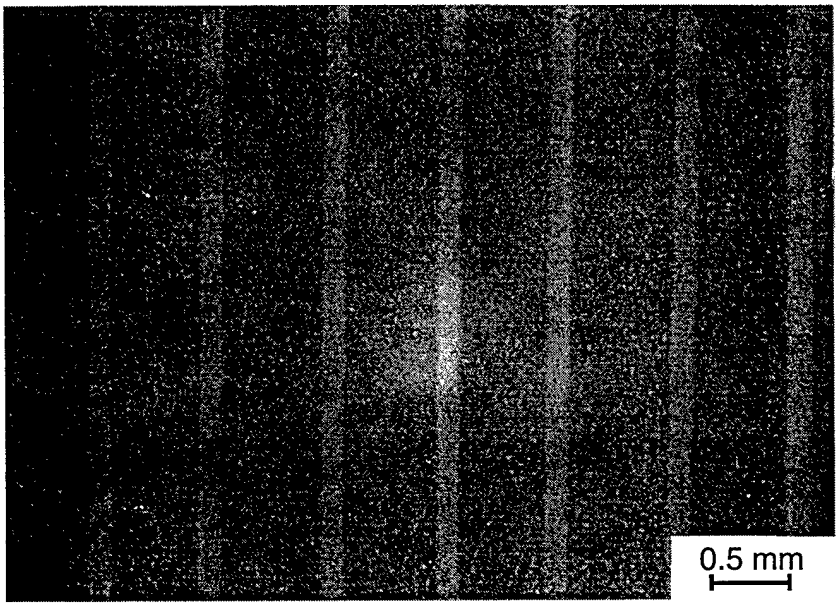

Fig. 3. Typical microstructure of laminates processed in this study. Micrograph shown is the 125 μm Nb/500 μm Nb_3Al laminate.

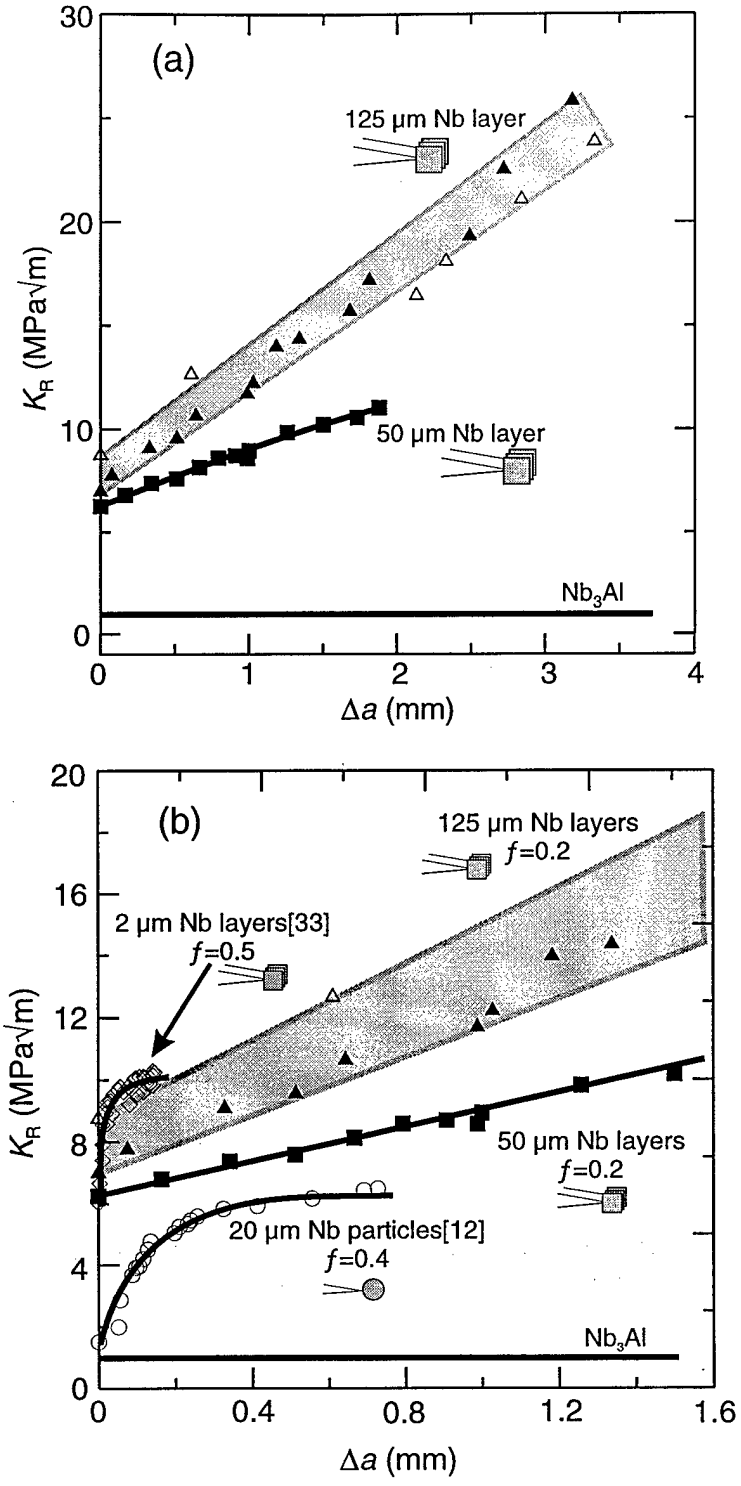

Fig. 4. a) Comparison of 50 μm thick Nb laminates indicating a significant influence of layer thickness on toughness. b) Comparison of coarser scale laminates of this study with microlaminated [33] and particle reinforced [12] Nb/Nb_3Al laminates showing improved toughness with the thickness layer laminates of this study.

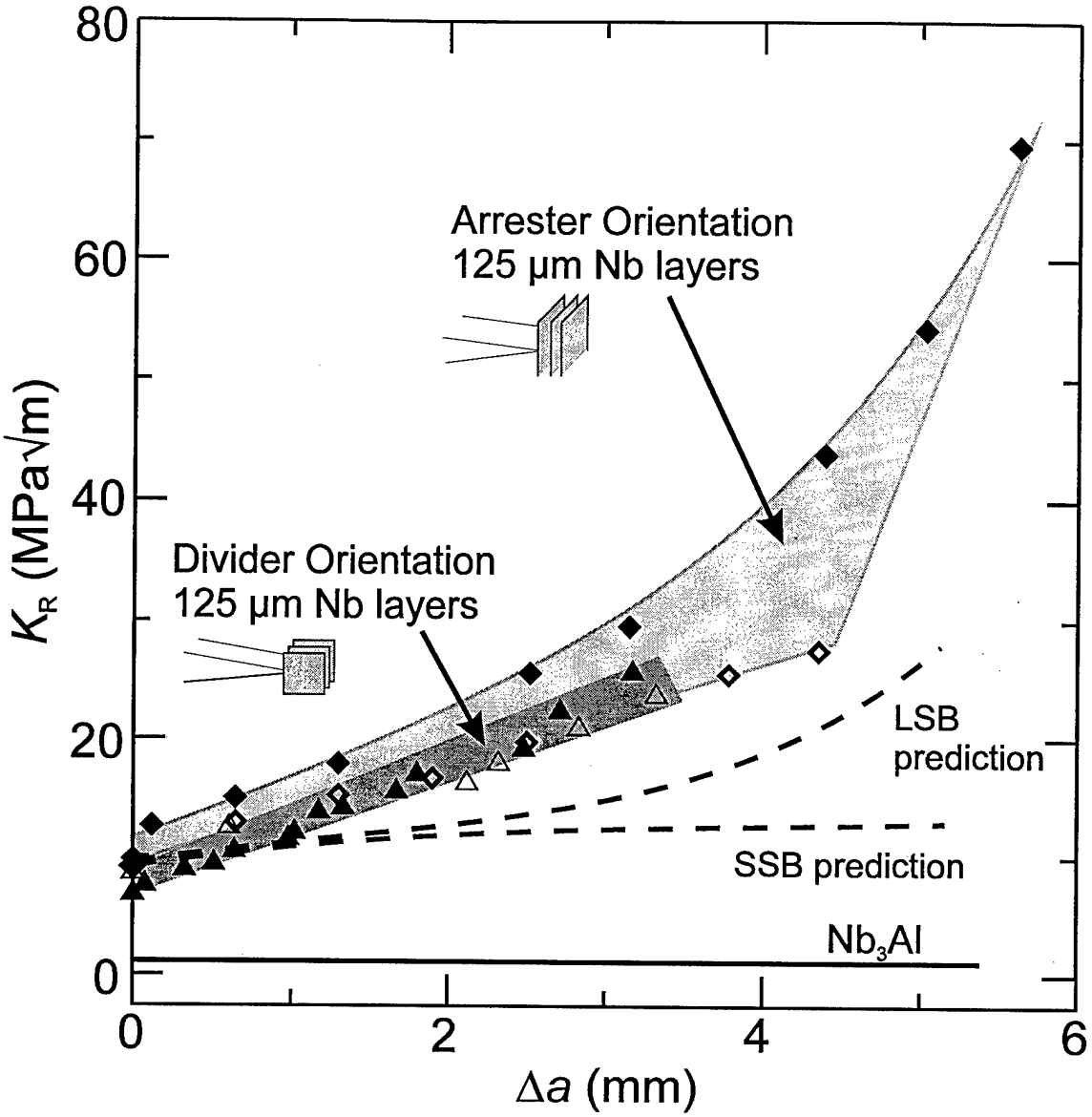

Fig. 5. Layer orientation affect on crack growth toughness. Large scale and small scale bridging predictions for arrester laminate shown as labeled.

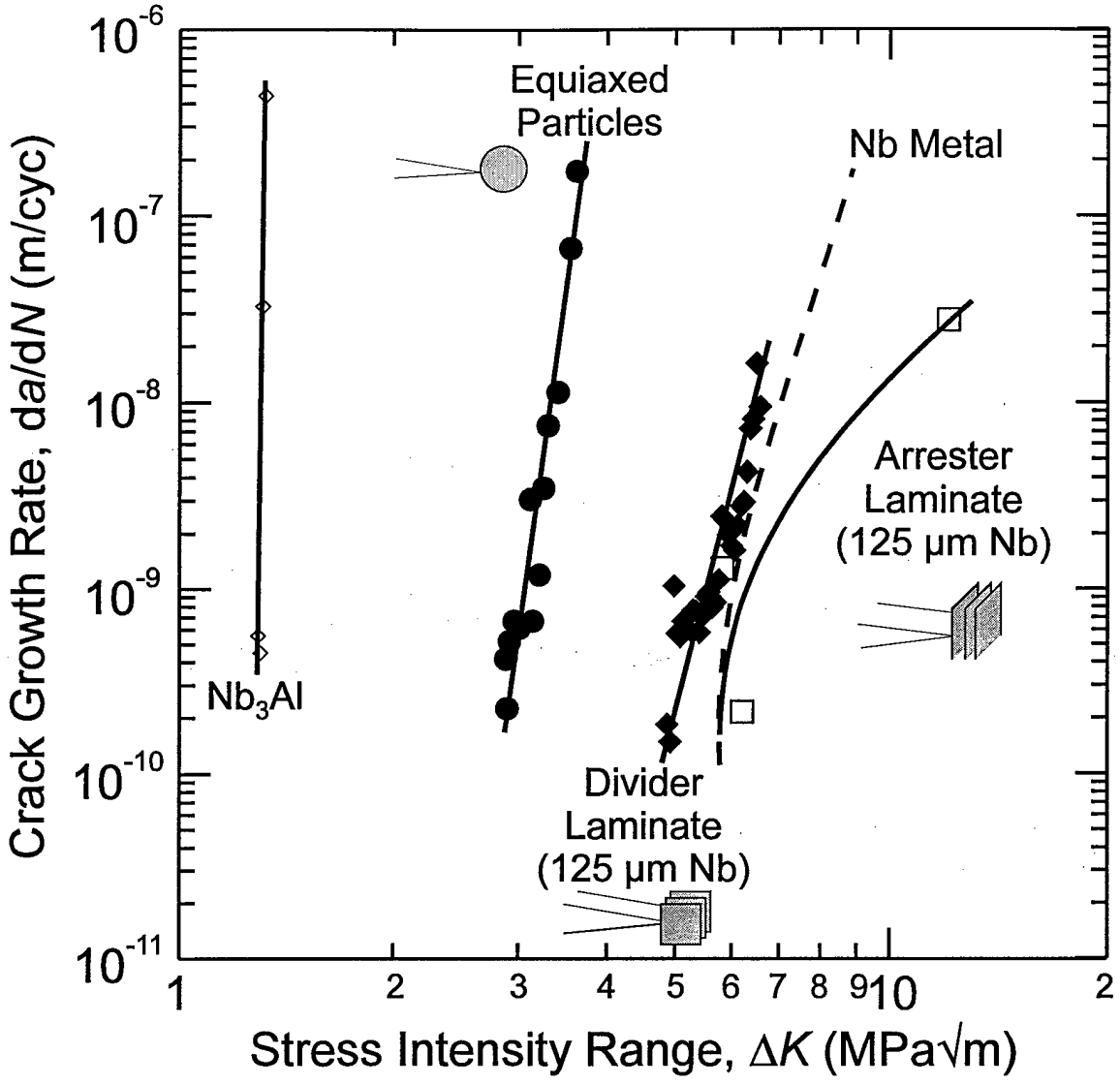

Fig. 6. Fatigue crack growth data demonstrating affect of reinforcement morphology and layer orientation.

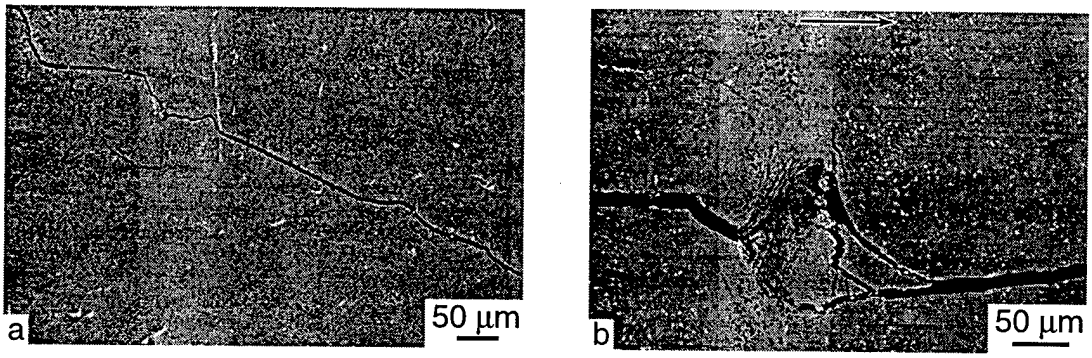

Fig. 7. a) Failure of Nb layer under fatigue crack growth conditions. b) Failure of Nb layer under monotonic loading conditions. Arrow indicates direction of crack growth.

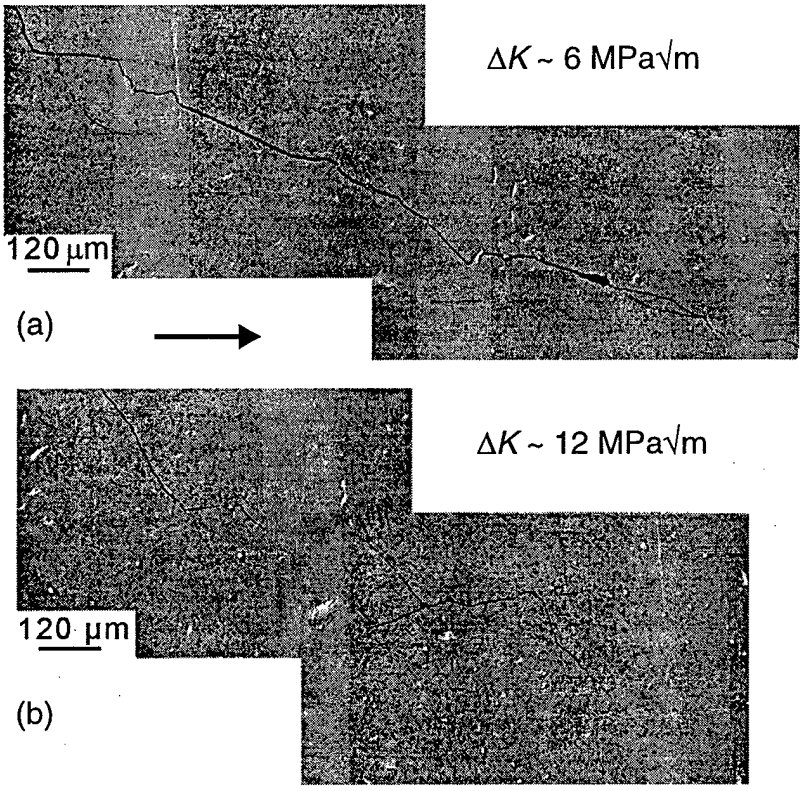

Fig. 8. a) Fatigue crack growing at low ΔK in arrester laminate. b) Fatigue crack growing at high ΔK in arrester laminate. Arrow indicates direction of crack growth.

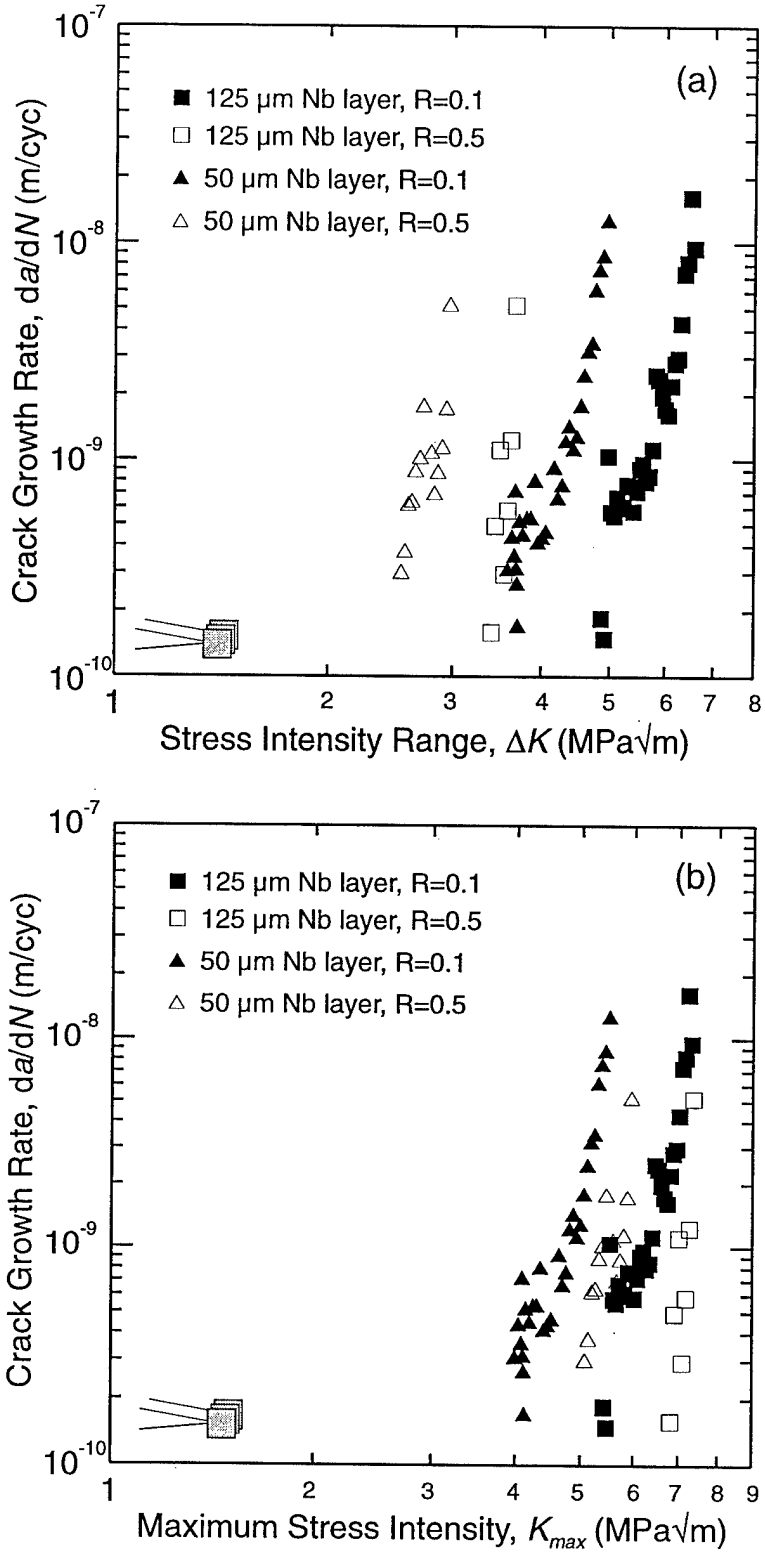

Fig. 9. a) Fatigue crack growth rate versus ΔK for divider laminate showing affect of layer thickness. b) Fatigue crack growth rate versus K_{max} showing relatively strong influence of K_{max} on fatigue crack growth rate.

8. PROGRAM ORGANIZATION AND PERSONNEL

The work described in this report was performed in the Department of Materials Science and Mineral Engineering, University of California at Berkeley, under the supervision of Dr. R. O. Ritchie, Professor of Materials Science, and Dr. K. T. Venkateswara Rao, Research Engineer, and aided by a graduate student research assistant working for his Ph.D. degree.

i) Professor R. O. Ritchie, Principal Investigator
Department of Materials Science and Mineral Engineering

ii) Dr. K. T. Venkateswara Rao, Co-Principal Investigator
Department of Materials Science and Mineral Engineering

iii) Don R. Bloyer, Graduate Student Research Assistant
Department of Materials Science and Mineral Engineering

9. PUBLICATIONS

9.1 Refereed Journals

1. D. R. Bloyer, K. T. Venkateswara Rao and R. O. Ritchie: "Resistance-Curve Toughening in Ductile/Brittle Layered Structures: Behavior in Nb/Nb_3Al Laminates," *Materials Science and Engineering A*, **216A** (1-2), Oct. 1996, pp. 80-90.

2. D. R. Bloyer, K. T. Venkateswara Rao and R. O. Ritchie, "Resistance-Curve Toughening in Ductile-Phase Intermetallic Laminates," in *The Johannes Weertman Symposium,* R. J. Arsenault, D. Cole, T. Gross, G. Kostorz, P. Liaw, S. Parameswaran, and H. Sizek, eds., TMS, Warrendale, PA, 1996, pp. 261-266.

3. D. R. Bloyer, K. T. Venkateswara Rao and R. O. Ritchie: "Toughness and Subcritical Crack Growth in Nb/Nb_3Al Layered Materials," in *Layered Materials for Structural Applications*, MRS Symposium Proceedings, J. J. Lewandowski, C. H. Ward, M. R. Jackson, and W. H. Hunt, Jr. (eds.), vol. 434, Materials Research Society, Pittsburgh, PA (1996), in press.

10. DISTRIBUTION LIST

AFOSR/NA
ATTN: Dr. C. H. Ward
110 Duncan Avenue, Suite B115
Bolling Air Force Base
Washington, D.C. 20332-8080

AFWAL/MLLM
ATTN: Branch Chief
Wright-Patterson AFB
Dayton, OH 45433

AFWAL/MLLS
ATTN: Branch Chief
Wright-Patterson AFB
Dayton, OH 45433

AFWAL/MLLN
ATTN: Branch Chief
Wright-Patterson AFB
Dayton, OH 45433

Dr. Hugh R. Gray
NASA Lewis Research Center
Materials and Structures Division
21000 Brookpark Rd.
Cleveland, OH 44135